Methionine-MAT2A-SAM axis controls lipid levels by regulating ACSL4

CHAOYI XIA and JINGSHU MIN

Zhejiang Provincial Engineering Research Center of New Technologies and Applications for Targeted Therapy of Major Diseases, College of Life Sciences and Medicine, Zhejiang Sci-Tech University, Hangzhou, Zhejiang 310018, P.R. China

Received March 31, 2025; Accepted July 4, 2025

DOI: 10.3892/ol.2025.15297

Abstract. The four major metabolic pathways in cells, including amino acid, glucose, nucleotide and lipid metabolism, constitute the fundamental framework of cellular metabolic networks. However, the intricate reciprocal regulatory mechanisms between amino acid metabolism and lipid metabolism remain poorly understood. In the present study, an essential amino acid-deficient culture medium was established and applied to cell cultures. Subsequent analysis using flow cytometry demonstrated that methionine deprivation significantly reduced cellular lipid accumulation and impaired the fatty acid uptake capacity. Mechanistic investigations using western blotting revealed that the methionine-methionine adenosyltransferase 2A (MAT2A)-S-adenosylmethionine (SAM) metabolic axis regulates the protein expression of ACSL4, a critical enzyme governing fatty acid uptake. Notably, the results indicated that the protein expression of MAT2A may be tightly regulated by SAM through a feedback mechanism, ensuring homeostasis of the methionine-MAT2A-SAM metabolic axis. In summary, the findings of the present study demonstrate that the methionine-MAT2A-SAM axis modulates lipid metabolism by regulating ACSL4 expression and function.

Introduction

Metabolism serves as the fundamental basis of cellular life, providing energy for biological processes, enabling the biosynthesis of macromolecules and maintaining redox homeostasis (1). The cellular metabolic network, comprising the four core pathways, amino acid, glucose, lipid and nucleotide metabolism, forms the structural and functional foundation of cellular biochemistry (2). Amino acid metabolism occupies a particularly pivotal position within this network due to its notable diversity in molecular species and metabolic routes, enabling its critical involvement in multiple cellular processes (3-8). Emerging evidence has revealed that deficiencies in essential amino acids, including tryptophan, tyrosine, branched-chain amino acids (such as isoleucine, leucine and valine), methionine, phenylalanine and threonine, can disrupt lipid homeostasis, with potential implications for neurodevelopmental disorders (9). In diabetic murine models, depletion of serine and glycine has been demonstrated to exacerbate neuropathy progression (10). A mechanistic study has further shown that essential amino acid deficiency in hepatocytes leads to functional impairment of ubiquitin protein ligase E3 component n-recognin 1, causing aberrant ubiquitination and subsequent degradation of the lipid droplet-stabilizing protein, perilipin 2. This molecular cascade ultimately suppresses hepatic lipid catabolism and promotes fatty liver pathogenesis (11).

To sustain their rapid proliferation, tumor cells must overcome three fundamental metabolic demands: i) Rapid energy production; ii) biosynthesis of macromolecules; and iii) maintenance of redox homeostasis (1). Amino acids serve as essential providers of both carbon and nitrogen sources, playing pivotal roles in meeting these metabolic challenges. Consequently, amino acid restriction therapies have emerged as a promising therapeutic strategy against tumors (12-17). Notably, the sulfur-containing amino acid, cysteine, assumes particular importance in tumor metabolism, serving as a critical precursor for glutathione (GSH) synthesis and providing cellular protection against ferroptosis (18,19). Ferroptosis is an iron-dependent form of regulated cell death characterized by three key metabolic features: i) The glutathione peroxidase 4/GSH antioxidant system (dependent on cysteine availability); ii) Fe^{2+}-mediated Fenton reactions; and iii) acyl-CoA synthetase long chain family member 4 (ACSL4)-catalyzed biosynthesis of polyunsaturated fatty acid-containing phospholipids (PUFA-PLs) (20). Notably, cellular cysteine can be acquired through two distinct pathways: Exogenous uptake via the solute carrier family 7 member 11 (SLC7A11) transporter or endogenous synthesis from methionine via the methionine adenosyltransferase 2A (MAT2A)-initiated transsulfuration pathway. Both SLC7A11 and MAT2A are

Correspondence to: Dr Chaoyi Xia, Zhejiang Provincial Engineering Research Center of New Technologies and Applications for Targeted Therapy of Major Diseases, College of Life Sciences and Medicine, Zhejiang Sci-Tech University, 928 Second Street, Xiasha Higher Education Park, Hangzhou, Zhejiang 310018, P.R. China
E-mail: xiacy834@zstu.edu.cn

Key words: methionine, S-adenosylmethionine, acyl-CoA synthetase long chain family member 4, fatty acid uptake

frequently upregulated in tumors, making them attractive therapeutic targets (21-25). Notably, ACSL4 plays a contradictory role in the occurrence and development of tumors. On the one hand, ACSL4 can provide biomacromolecules for tumor proliferation by regulating the synthesis of PUFA-PLs (26). On the other hand, an increase in PUFA-PLs levels also increases the sensitivity of tumor cells to ferroptosis (27). Beyond their canonical roles in protein biosynthesis and cellular metabolism, amino acids serve as pivotal allosteric modulators that fine-tune metabolic flux through the direct regulation of rate-limiting enzymes (28). While the crosstalk between amino acid metabolism and glucose homeostasis has been extensively characterized, particularly through the dynamic interconversion of non-essential amino acid networks, the unidirectional nature of amino acid-lipid metabolic interactions has resulted in comparatively limited understanding of the amino acid-mediated regulation of lipid metabolism.

The present study aimed to systematically investigate the metabolic consequences of essential amino acid deprivation, with particular emphasis on delineating the mechanistic role of methionine in regulating intracellular lipid homeostasis. To assess alterations in lipid metabolism, flow cytometry coupled with fluorescent lipid probes were employed to evaluate intracellular lipid accumulation and cellular fatty acid uptake efficiency following essential amino acid deprivation. Comprehensive analyses were performed to elucidate the underlying molecular mechanisms of methionine-mediated lipid metabolic regulation. Western blotting and reverse transcription-quantitative PCR (RT-qPCR) were conducted to examine methionine restriction-induced modulation of ACSL4 expression, a critical regulator of fatty acid metabolism (27). Furthermore, the feedback regulation within the methionine-MAT2A-S-adenosylmethionine (SAM) metabolic axis was systematically investigated through combined western blotting and RT-qPCR analyses, with a specific focus on the SAM-dependent regulation of MAT2A protein stability and its consequent impact on lipid metabolic homeostasis.

Materials and methods

Cell culture. Mouse embryonic fibroblasts (MEFs) (CRL-2991; ATCC) and the HT1080, DU145 and H1299 cell lines were obtained from the American Tissue Culture Collection (ATCC) and cultured following ATCC recommendations. These cells were also subjected to STR identification and mycoplasma testing. The cells were sustained in Dulbecco's modified Eagle's medium (DMEM) with high glucose, sodium pyruvate (1 mM), glutamine (2 mM), penicillin (100 U/ml), streptomycin (0.1 mg/ml) and 10% (v/v) fetal bovine serum (FBS; MeisenCTCC; Zhejiang Meisen Cell Technology Co., Ltd.) at 37˚C and 5% CO_2. In addition, the cultivation conditions for methionine deficiency are based on DMEM (cat. no. D0422; MilliporeSigma) with high glucose, sodium pyruvate (1 mM), glutamine (2 mM), penicillin (100 U/ml), streptomycin (0.1 mg/ml) and 10% (v/v) fetal bovine serum (FBS) (MeisenCTCC) at 37˚C and 5% CO_2. Alternatively, S-adenosylmethionine (SAM; 0.4 mM), S-adenosylhomocysteine (SAH; 0.4 mM), homocysteine (Hcy; 0.4 mM) or adenosine dialdehyde (ADOX; 0.4 mM) were added separately to methionine deficient culture medium to treat cells. Cells were also treated with a constructed culture medium lacking essential amino acids (isoleucine, 0.4 mM; isoleucine, 0.4 mM; lysine, 0.4 mM; methionine, 0.4 mM; phenylalanine, 0.4 mM; threonine, 0.4 mM; tryptophan, 0.4 mM; valine, 0.4 mM; histidine, 0.4 mM; and arginine, 0.4 mM).

Reagents. The reagents used included propidium iodide (PI; cat. no. P4170; MilliporeSigma), BODIPY581/591 C11 (cat. no. D3861; Thermo Fisher Scientific, Inc.), BODIPY (cat. no. HY-D1614; MedChemExpress), BODIPY™ FL C12 (cat. no. D3822; Thermo Fisher Scientific, Inc.), SAM (cat. no. A7007; MilliporeSigma), S-Adenosylhomocysteine (SAH; cat. no. A9384; MilliporeSigma), homocysteine (cat. no. H4628; MilliporeSigma), anti-MAT2A (cat. no. A19272; ABclonal Biotech Co., Ltd.), anti-ACSL4 (cat. no. A20414; ABclonal Biotech Co., Ltd.) and DMEM with high glucose (cat. no. D0422-100 ml; MilliporeSigma). In addition, all the components of the D777 culture medium (with 4,500 mg/l glucose, L-glutamine and sodium pyruvate, without sodium bicarbonate, powder, suitable for cell culture) were purchased to construct an amino acid-deficient culture medium. The medium mainly included methionine (cat. no. M0960000), leucine (cat. no. L8000), isoleucine (cat. no. I2752), lysine (cat. no. L5501), phenylalanine (cat. no. P17008), tyrosine (cat. no. T1145), tryptophan (cat. no. T0254), valine (cat. no. V0500), histidine (cat. no. H8125) and arginine (cat. no. A5006), all from MilliporeSigma.

Fatty acid uptake and intracellular lipid detection. Fatty acid uptake was measured by flow cytometry. Briefly, HT1080 and H1299 cells were plated at a density of $5x10^4$ cells per well in a 24-well dish and cultured for 12 h in DMEM supplemented with 10% FBS, 1% penicillin and streptomycin at 37˚C with 5% CO_2. Subsequently, 2 μM BODIPY-C12 was added to the cell culture medium and incubated for 10 h alongside the indicated treatment. Following this, the cells were trypsinized, washed with PBS containing 5% FBS and resuspended in 0.3 ml of PBS with 5% FBS for flow cytometry analysis (Attune NxT; Thermo Fisher Scientific, Inc.). Acquired data were analyzed using FlowJo version 10 software (FlowJo LLC). A minimum of 10,000 cells were analyzed per condition. Intracellular lipids were also measured by flow cytometry (Attune NxT.). Acquired data were analyzed using FlowJo version 10 software. The protocol was the same as that aforementioned except 1 μg/ml BODIPY was added to the cell culture medium and incubated for 30 min after the indicated treatment.

Lipid reactive oxygen species (ROS) detection. Lipid ROS were analyzed by flow cytometry. Briefly, cells were plated at a density of $1x10^5$ cells per well in a 24-well dish and cultured overnight in DMEM. Subsequently, 4 μM BODIPY581/591 C11 was added to the cell culture medium and incubated for 30 min after the indicated treatment. Excess BODIPY581/591 C11 was then removed by washing the cells with PBS twice. Labeled cells were trypsinized and resuspended in PBS with 5% FBS. Oxidation of BODIPY581/591 C11 resulted in a shift of the fluorescence emission peak from 590 to 510 nm

proportional to the lipid ROS generation, which was detected using a flow cytometer (Attune NxT). Acquired data were analyzed using FlowJo version 10 software.

Cell death detection. Cell death was analyzed by flow cytometry. Briefly, cells were plated at a density of $2x10^5$ cells per well in a 12-well dish for 12 h in fresh medium. After the indicated treatment, 1 μg/ml PI was added to the cell culture medium and incubated for 30 min. Then, cells were trypsinized, washed with PBS containing 5% FBS and resuspended in 0.3 ml of PBS with 5% FBS for flow cytometry (Attune NxT). Acquired data were analyzed using FlowJo software.

Apoptosis detection. Apoptosis was analyzed by flow cytometry. Briefly, cells were plated in 12-well culture plates at a density of $1x10^5$ cells per well and cultured in DMEM for 12 h. Cells were then trypsinized, washed with PBS containing 5% FBS and resuspended in 0.3 ml of PBS. Subsequently, PI and Annexin V-FITC were added to the cells and incubated for 30 min, and cell apoptosis was detected by flow cytometry (Attune NxT). Acquired data were analyzed using FlowJo.

Transfections. Transfections were conducted using Lipofectamine™ 2000 transfection reagent (Invitrogen; Thermo Fisher Scientific, Inc.) according to the manufacturer's protocol. HT1080 cells seeded in a 6-well dish were transfected with 40 ng of the following small interfering RNAs (Suzhou GenePharma Co., Ltd.): NC (scrambled), sense: 5'-UUCUCCGAACGUGUCACGUUTT-3', antisense: 5'-AACGUGACACGUUCGGAGAATT-3'; MAT2A-1, sense: 5'-GGAUCGAGGUGCUGUGCUUTT-3', antisense: 5'AAGCACAGCACCUCGAUCCTT-3'; MAT2A-2, sense: 5'-GGGAUGCCCUAAAGGAGAATT-3', antisense: 5'-UUCUCCUUUAGGGCAUCCCTT-3' and MAT2A-3, sense: 5'-GCCUAUGGCCACUUUGGUATT-3', antisense: 5'-UACCAAAAGUGGCCAUAGGCTT-3'. After transfection, the cells were placed in a 37˚C cell culture incubator and the medium was changed after 8 h. After 48 h, the cells were lysed and the interference efficiency was measured using western blotting.

Western blotting. Cell lysate preparation, SDS-PAGE and electrophoretic transference were accomplished as previously described (19). Briefly, the protein sample was quantified using a NanoPhotometer® N30 Touch and each lane of the 8% SDS gel was loaded with 10 μg protein sample. Membranes were blocked with 5% non-fat dried milk in TBS (pH 7.2) containing 0.1% Tween 20 (TBST), incubated with the appropriate primary antibodies in 5% non-fat dried milk in TBST overnight at 4˚C. Then, the membrane was incubated with the appropriate secondary antibodies in 5% non-fat dried milk in TBST at room temperature for 50 min. The following primary antibodies were used: Anti-MAT2A, anti-ACSL4 and β-actin (cat. no. HC201-01; TransGen Biotech Co., Ltd.). The following secondary antibodies were used: HRP-conjugated goat anti-rabbit (cat. no. AS014; ABclonal Biotech Co., Ltd.) and HRP-conjugated goat anti-mouse (cat. no. AS003; ABclonal Biotech Co., Ltd.). Chemiluminescence was detected using the ChampChemi 610 (SinSage Technology Co., Ltd.), and the software used for densitometry was ImageJ (National Institutes of Health).

RT-qPCR. Total RNA was extracted from cells using TRNzol (cat. no. DP424; Tiangen Biotech Co., Ltd.) and reverse transcribed with the PrimeScript™ RT reagent Kit with gDNA Eraser (cat. no. RR047A; Takara Bio, Inc.) according to the manufacturer's protocol. The resulting cDNA was then subjected to qPCR using the TB Green Premix Ex Taq™ (Tli RNase H Plus) (cat. no. RR820A; Takara Bio, Inc.). The detection and analysis were accomplished as previously described (19). The sequences of the primers used for qPCR were as follows: ACSL4 (human) forward, 5'-CATCCCTGGAGCAGATACTCT-3' and reverse, 5'-TCACTTAGGATTTCCCTGGTCC-3'; MAT2A (human) forward, 5'-ACCAGAAAGTGGTTCGTGAAG-3' and reverse, 5'-CAAGGCTACCAGCACGTTACA-3'; MAT2B (human) forward, 5'-TTCACTGGTCTGGCAATGAAC-3' and reverse, 5'-AGGGCTGTCAGTAATAGGTCTT-3'; MAT2A (mouse) forward, 5'-GCTTCCACGAGGCGTTCAT-3' and reverse, 5'-AGCATCACTGATTTGGTCACAA-3'; MAT2B (mouse) forward, 5'-AGGGAACCTTTCACTGGTCTG-3' and reverse 5'-ATTTGGAGCAATCGAGCTGAG-3'; β-actin (human) forward, 5'-GTTGTCGACGACGAGCG-3' and reverse, 5'-GCACAGAGCCTCGCCTT-3'; and β-actin (mouse) forward, 5'-GGCTGTATTCCCCTCCATCG-3' and reverse, 5'-CCAGTTGGTAACAATGCCATGT-3'.

Public database analyses

ACLS4 expression in cancer. The expression levels of *ACSL4* in tumor and normal tissues were analyzed using the Expression DIY module on the GEPIA 2 website (http://gepia2.cancer-pku.cn/#index). The analysis parameter settings were as follows: Log2 FC cut-off (1); q-value cut-off (0.01); log scale (yes); jitter size (0.4); and matched normal data (match TCGA normal and GTEx data).

Overall survival. The survival analysis module on the GEPIA 2 website was used to analyze the relationship between ACSL4 expression and patient survival. The analysis parameter settings were as follows: Methods (overall survival); group cut-off (median); cut-off high (%) (50); cut-off low (%) (50); hazard ratio (yes); 95% confidence interval (yes); and axis units (months).

Statistical analysis. GraphPad Prism (v.10.4.0; Dotmatics) software was used to calculate the P-values using two-sided unpaired t-test or one-way ANOVA followed by Tukey's Honestly Significant Difference. All data presented in the figures represent the mean ± SD. $P<0.05$ was considered to indicate a statistically significant difference.

Results

Methionine restriction downregulates cellular lipid levels. To systematically evaluate the role of essential amino acids in lipid metabolism regulation, an essential amino acid-deficient culture system was established by excluding leucine, isoleucine, lysine, methionine, phenylalanine, tyrosine, tryptophan, valine, histidine and arginine from the medium. HT1080 cells cultured in this modified medium were subsequently analyzed for intracellular lipid accumulation using BODIPY staining. Quantitative analysis revealed that methionine deprivation specifically caused a significant reduction in cellular lipid content (Fig. 1A). Next, the functional consequences of

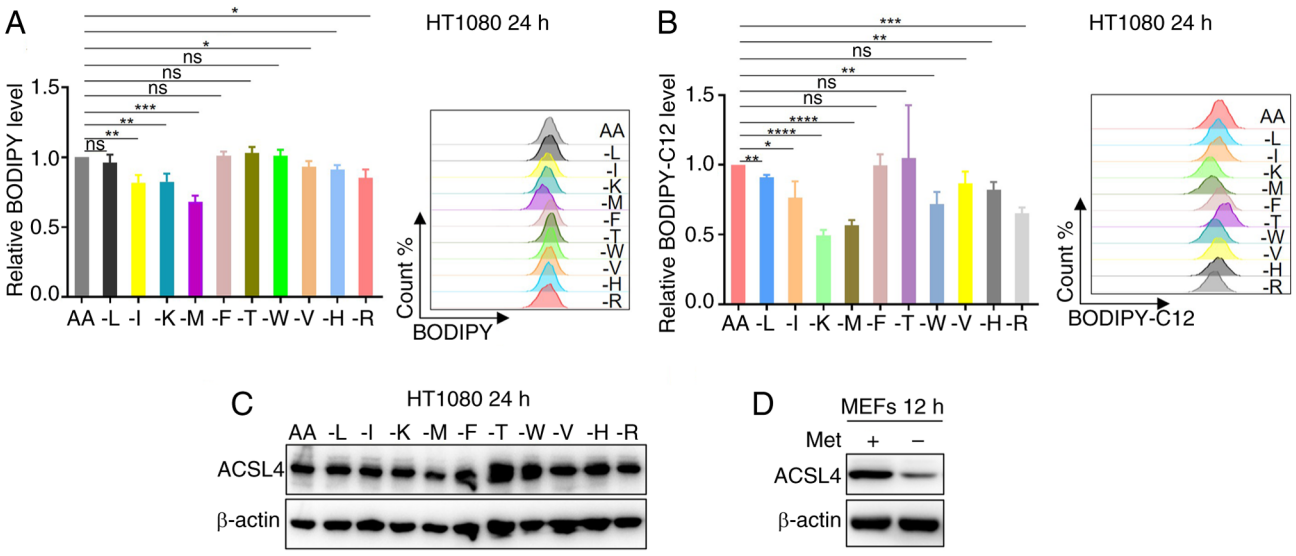

Figure 1. Methionine restriction downregulates cellular lipid levels. (A) HT1080 cells were cultured without leucine, isoleucine, lysine, methionine, phenylalanine, tyrosine, tryptophan, valine, histidine or arginine as indicated for 24 h, and the intracellular lipids were determined by BODIPY staining coupled with flow cytometry (n=3). (B) HT1080 cells were cultured without leucine, isoleucine, lysine, methionine, phenylalanine, tyrosine, tryptophan, valine, histidine, or arginine as indicated for 24 h, and fatty acid uptake capacity was determined by BODIPY-C12 staining coupled with flow cytometry (n=3). (C) Western blot analysis of ACSL4 expression in HT1080 cells treated with medium without leucine, isoleucine, lysine, methionine, phenylalanine, tyrosine, tryptophan, valine, histidine or arginine as indicated for 24 h. (D) Western blot analysis of ACSL4 expression in MEFs cells treated with medium without methionine for 12 h. Data are presented as the mean ± SD with P-values determined by one-way ANOVA followed by Tukey's Honestly Significant Difference. *P<0.05, **P<0.01, ***P<0.001, ****P<0.0001. AA, all amino acids; L, isoleucine; I, isoleucine; K, lysine; M, methionine; F, phenylalanine; T, threonine; W, tryptophan; V, valine; H, histidine; R, arginine; ACSL4, acyl-CoA synthetase long chain family member 4; MEFs, mouse embryonic fibroblasts; Met, methionine.

essential amino acid deficiency on fatty acid uptake capacity were examined using BODIPY-C12 fluorescence assays. Notably, methionine-deficient conditions produced a notable impairment in fatty acid internalization among all tested amino acid deprivations (Fig. 1B).

Given the established role of ACSL4 in facilitating fatty acid uptake through its dual function of converting fatty acids to acyl-CoA derivatives and inhibiting fatty acid efflux, ACSL4 protein expression in HT1080 cells under essential amino acid deprivation conditions was first examined. Western blot analysis revealed that methionine deficiency reduced the ACSL4 protein levels (Fig. 1C). To validate this finding across different cellular contexts, the investigation was extended to MEFs under methionine-restricted conditions. Consistent with the initial observation, methionine deprivation significantly decreased ACSL4 expression in MEFs cells (Fig. 1D). Taken together, the results suggest that methionine deficiency attenuates cellular lipid accumulation and the fatty acid uptake capacity, potentially through downregulation of ACSL4 protein expression, revealing a novel mechanistic link between methionine availability and lipid metabolic regulation.

Methionine regulates ACSL4 through SAM. As the sulfur-containing amino acid methionine functions as a vital cellular methyl donor primarily through its metabolic derivative SAM, it was next determined whether methionine regulates ACSL4 expression and fatty acid uptake capacity via SAM-dependent mechanisms. To test this hypothesis, methionine deprivation experiments in HT1080 cells were performed followed by SAM supplementation. Western blot analysis demonstrated that SAM administration rescued

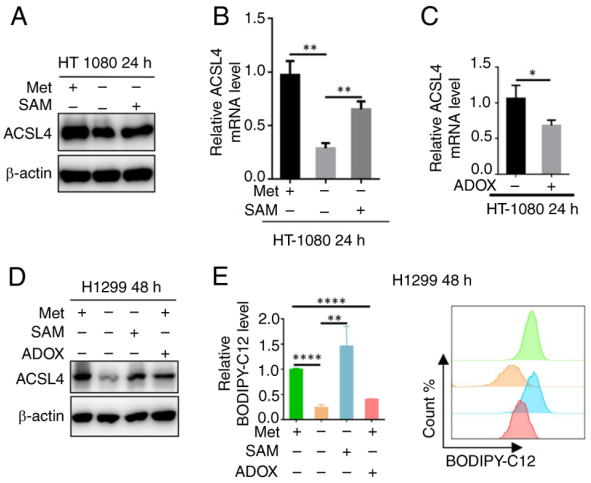

Figure 2. Methionine regulates ACSL4 through SAM. (A) Western blot analysis of ACSL4 expression in HT1080 cells cultured ± methionine or ± SAM as indicated for 24 h. The *ACSL4* mRNA levels in HT1080 cells cultured (B) ± methionine and ± SAM (C) or ± ADOX as indicated for 24 h were analyzed using reverse transcription-quantitative PCR (n=3). (D) Western blot analysis of ACSL4 expression in H1299 cells cultured ± methionine, ± SAM or ± ADOX as indicated for 48 h. (E) H1299 cells were cultured ± methionine, ± SAM or ± ADOX as indicated for 48 h, and fatty acid uptake capacity was determined by BODIPY-C12 staining coupled with flow cytometry (n=3). Data are presented as mean ± SD with P-values determined by one-way ANOVA followed by Tukey's Honestly Significant Difference. *P<0.05, **P<0.01, ****P<0.0001. ACSL4, acyl-CoA synthetase long chain family member 4; SAM, S-adenosylmethionine; ADOX, adenosine dialdehyde; Met, methionine.

the methionine deficiency-induced reduction in ACSL4 protein levels (Fig. 2A). Complementary RT-qPCR analysis further revealed that SAM supplementation similarly

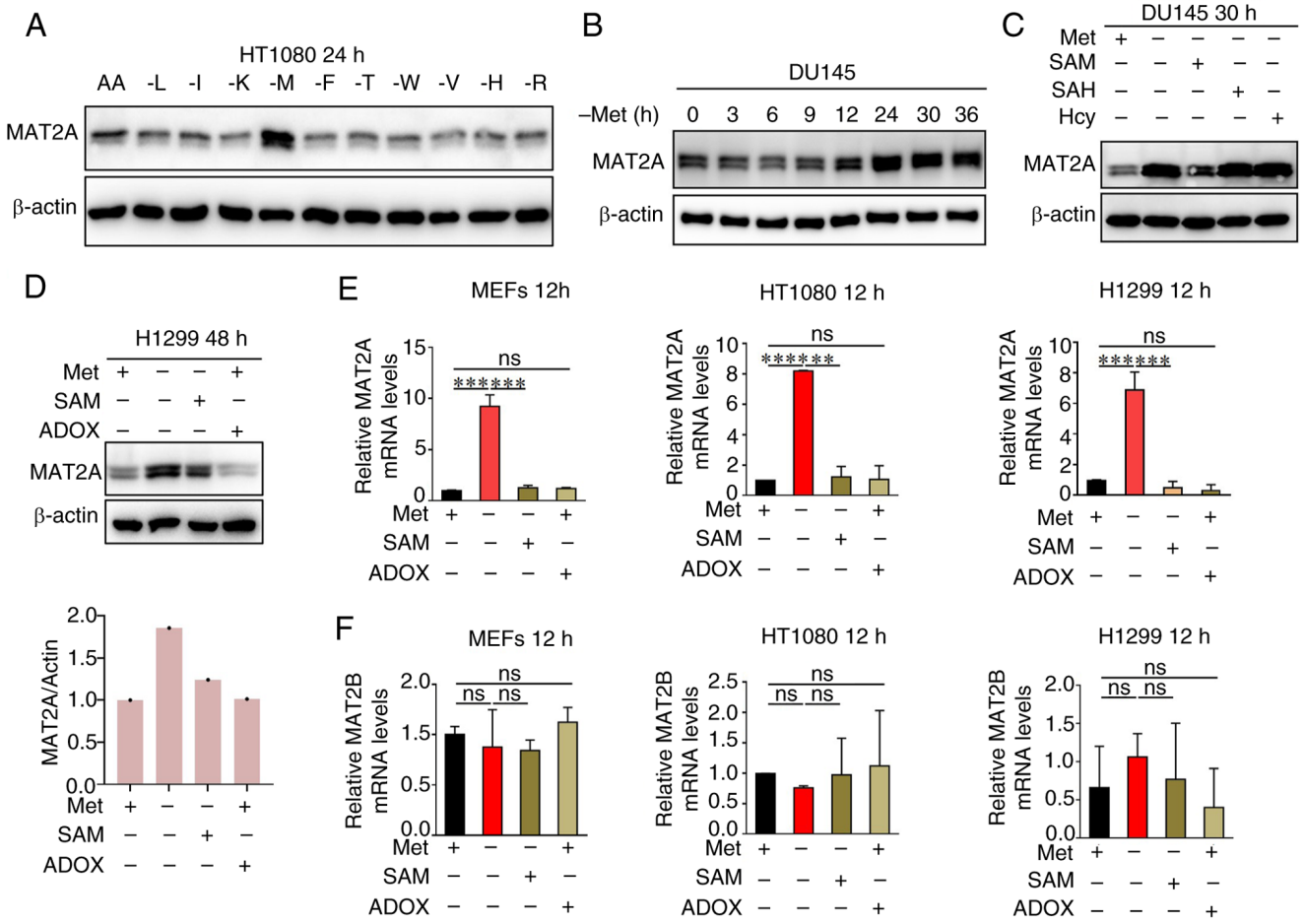

Figure 3. MAT2A can be dynamically regulated by the level of SAM. (A) Western blot analysis of MAT2A expression in HT1080 cells treated with medium without leucine, isoleucine, lysine, methionine, phenylalanine, tyrosine, tryptophan, valine, histidine, or arginine as indicated for 24 h. (B) Western blot analysis of MAT2A expression in DU145 cells treated with medium without methionine as indicated for 0, 3, 6, 9, 12, 24, 30 and 36 h. (C) Western blot analysis of MAT2A expression in DU145 cells cultured ± methionine, ± SAM, ± SAH or ± Hcy as indicated for 30 h. (D) Western blot analysis of MAT2A expression in H1299 cells cultured ± methionine, ± SAM or ± ADOX, as indicated for 48 h. The (E) *MAT2A* and (F) *MAT2B* mRNA levels in MEFs and HT1080 and H1299 cells cultured ± methionine, ± SAM or ± ADOX as indicated for 12 h, were analyzed using reverse transcription-quantitative PCR (n=3). Data are presented as mean ± SD with P-values determined by one-way ANOVA followed by Tukey's Honestly Significant Difference. **P<0.01, ***P<0.001, ****P<0.0001. ns, non-significant; AA, all amino acids; L, isoleucine; I, isoleucine; K, lysine; M, methionine; F, phenylalanine; T, threonine; W, tryptophan; V, valine; H, histidine; R, arginine; MEFs, mouse embryonic fibroblasts; SAM, S-adenosylmethionine; ADOX, adenosine dialdehyde; SAH, S-adenosylhomocysteine; Hcy, homocysteine; MAT2A/B, methionine adenosyltransferase 2A/B; Met, methionine.

restored the suppressed *ACSL4* mRNA expression under methionine-depleted conditions (Fig. 2B). To elucidate whether SAM regulates ACSL4 expression through methylation-dependent mechanisms, HT1080 cells were treated with the methylation inhibitor, adenosine dialdehyde (ADOX), and the *ACSL4* transcript levels were analyzed. RT-qPCR analysis revealed that ADOX treatment significantly suppressed *ACSL4* mRNA expression (Fig. 2C), indicating methylation-dependent regulation. This regulatory mechanism in H1299 cells was further validated, as western blot analysis confirmed that the methionine-SAM axis controls ACSL4 protein abundance possibly through methylation modifications (Fig. 2D). Functional assays demonstrated that this methylation-dependent regulation directly impacts cellular fatty acid uptake capacity (Fig. 2E). Collectively, these results establish that SAM-mediated methylation may represent a critical epigenetic mechanism through which methionine regulates *ACSL4* expression and function in lipid metabolism.

MAT2A can be dynamically regulated by the level of SAM. As the key enzyme catalyzing methionine-to-SAM conversion, MAT2A occupies a central position in the methionine-SAM metabolic axis (24). To investigate whether MAT2A serves as a critical regulator of SAM homeostasis and lipid metabolism, MAT2A protein expression in HT1080 cells under essential amino acid deprivation was first examined. Western blot analysis revealed that the MAT2A levels were specifically upregulated by methionine deficiency (Fig. 3A). Using a dose-response approach, it was demonstrated that MAT2A expression exhibits sensitivity to extracellular methionine concentrations in DU145 cells (Fig. 3B). Notably, SAM supplementation reversed the observed methionine deprivation-induced MAT2A upregulation (Fig. 3C), suggesting a feedback regulatory mechanism. Further mechanistic studies in H1299 cells showed that MAT2A protein levels remained unchanged following ADOX-mediated methylation inhibition, compared with the methionine deprivation only group (Fig. 3D). Consistent with this result, transcriptional analysis

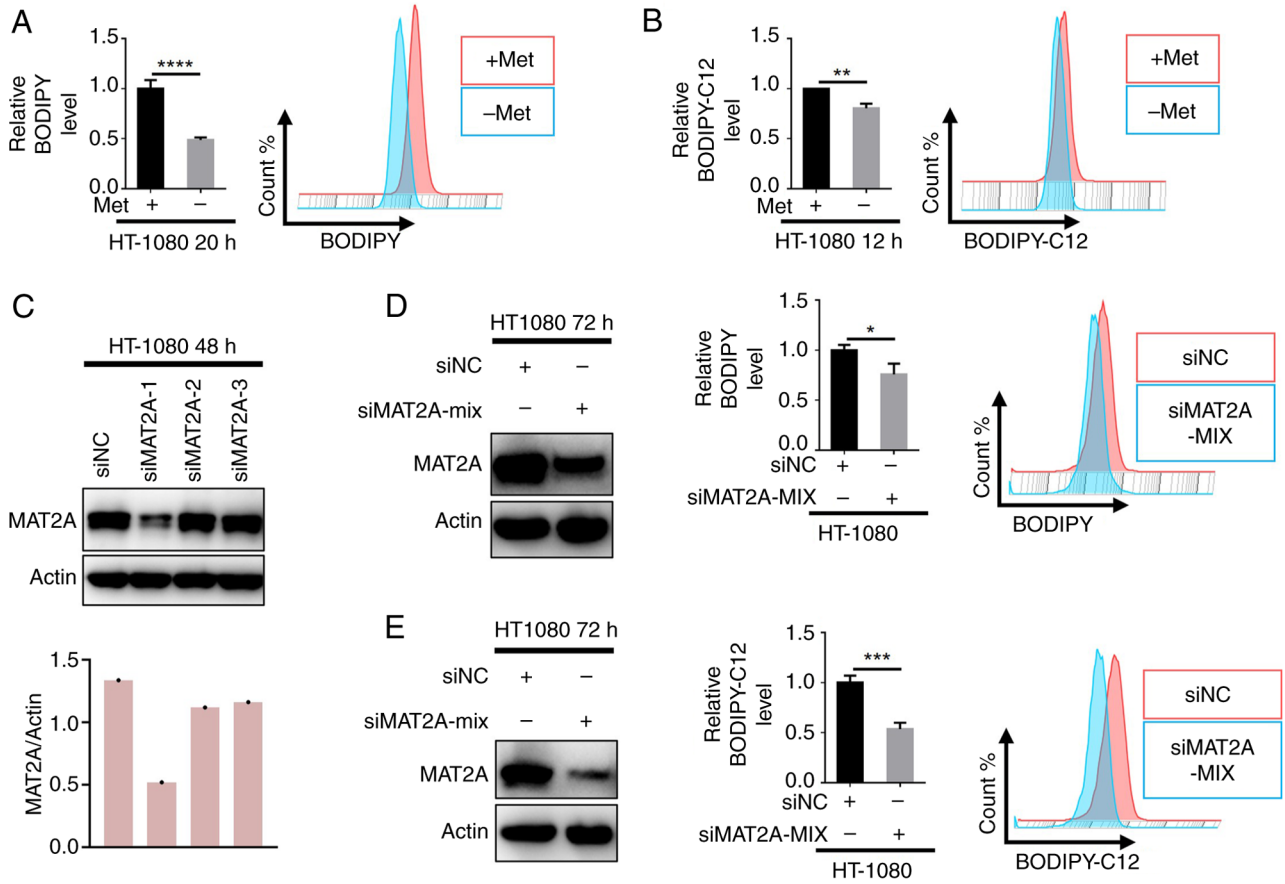

Figure 4. Knocking down MAT2A expression reduces the intracellular lipid levels. (A) HT1080 cells were cultured ± methionine as indicated for 20 h, and the intracellular lipids were determined by BODIPY staining coupled with flow cytometry (n=3). (B) HT1080 cells were cultured ± methionine as indicated for 12 h, and fatty acid uptake capacity was determined by BODIPY-C12 staining coupled with flow cytometry (n=3). (C) Western blot analysis of MAT2A expression in HT1080 cells transfected with siMAT2A or siNC. (D) The intracellular lipids in HT1080 cells transfected with siMAT2A or siNC were determined by BODIPY staining coupled with flow cytometry (n=3). (E) Fatty acid uptake capacity in HT1080 cells transfected with siMAT2A or siNC was determined by BODIPY-C12 staining coupled with flow cytometry (n=3). Data are presented as mean ± SD, with P-values determined by one-way ANOVA followed by Tukey's Honestly Significant Difference. *P<0.05, **P<0.01, ***P<0.001, ****P<0.0001. MAT2A, methionine adenosyltransferase 2A; si, small interfering (RNA); NC, negative control; Met, methionine.

across multiple cell lines (MEFs, HT1080 and H1299) revealed that, while the methionine-SAM axis regulates *MAT2A* mRNA expression, this control occurs independently of the methyltransferase activity of SAM (Fig. 3E). Notably, the regulatory subunit, MAT2B, was unaffected by these metabolic perturbations (Fig. 3F). These results establish that MAT2A is subject to SAM-mediated feedback regulation through a novel methylation-independent mechanism, highlighting the sophisticated control of methionine metabolism.

Knocking down MAT2A reduces intracellular lipid levels. To systematically validate the regulatory role of methionine in lipid metabolism, complementary experimental approaches were performed using HT1080 cells. First, methionine deprivation (using commercial methionine deficient medium) led to significant reductions in both intracellular lipid accumulation (BODIPY staining) and fatty acid uptake capacity (BODIPY-C12 assay) (Fig. 4A and B). To directly assess the involvement of MAT2A in these metabolic processes, RNA interference-mediated knockdown was employed. MAT2A downregulation similarly reduced the intracellular lipid content (Fig. 4C and D) and impaired fatty acid internalization (Fig. 4E), phenocopying the effects of methionine deprivation. These consistent findings across orthogonal experimental approaches establish MAT2A as a key metabolic regulator and potential therapeutic target for modulating cellular lipid homeostasis.

Methionine restriction suppresses tumor cell proliferation by inhibiting ACLS4. Lipids serve as fundamental structural components of cellular membranes and play a critical role in supporting the rapid proliferation of tumor cells. The aforementioned results demonstrated that methionine functions as a positive regulator of intracellular lipid homeostasis. Analysis of The Cancer Genome Atlas datasets revealed elevated *ACSL4* expression in multiple malignancies, including esophageal carcinoma, liver hepatocellular carcinoma, pancreatic adenocarcinoma and stomach adenocarcinoma (Fig. 5A). Notably, high *ACSL4* expression was significantly associated with poorer overall survival in patients with cancer, including cholangiocarcinoma, esophageal carcinoma and colon adenocarcinoma (Fig. 5B), suggesting its clinical relevance as a potential prognostic marker. Functional studies in HT1080 cells showed that methionine deprivation simultaneously

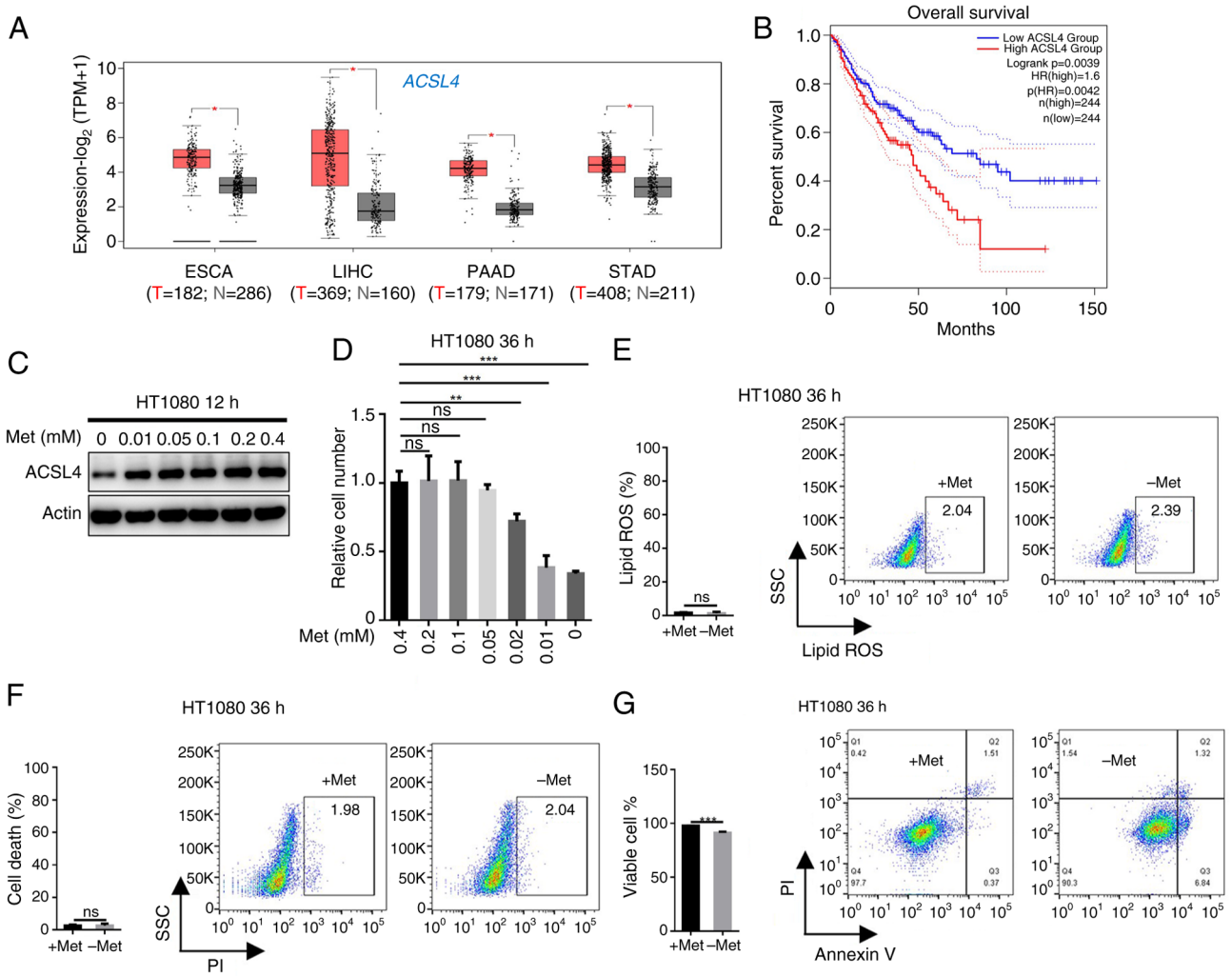

Figure 5. Methionine restriction suppresses tumor cell proliferation by inhibiting ACLS4. (A) Analysis of *ACSL4* expression in tumor and adjacent tissues based on TCGA database. (B) Analysis of the correlation between ACSL4 expression and overall survival based on TCGA database through GEPIA2 (http://gepia2.cancer-pku.cn/). (C) Western blot analysis of ACSL4 expression in HT1080 cells treated with medium without methionine as indicated for 12 h. (D) The number of HT1080 cells after methionine deprivation as indicated for 36 h were counted using a microscope and cell counter (n=3). (E) HT1080 cells were cultured ± methionine as indicated for 36 h and the lipid ROS level was determined by BODIPY-C11 staining coupled with flow cytometry (n=3). (F) HT1080 cells were cultured ± methionine as indicated for 36 h and cell death was determined by PI staining coupled with flow cytometry (n=3). (G) HT1080 cells were cultured ± methionine as indicated for 36 h and cell apoptosis was determined by PI staining coupled with flow cytometry (n=3). Data are presented as mean ± SD, with P-values determined by one-way ANOVA followed by Tukey's Honestly Significant Difference. *P<0.05, **P<0.01, ***P<0.001. ns, non-significant; TCGA, The Cancer Genome Atlas; TPM, transcripts per million; ESCA, esophageal carcinoma; LIHC, liver hepatocellular carcinoma; PAAD, pancreatic adenocarcinoma; STAD, stomach adenocarcinoma; T, tumor; N, normal; HR, hazard ratio; ACSL4, acyl-CoA synthetase long chain family member 4; SSC, side Scatter; ROS, reactive oxygen species; PI, propidium iodide; Met, methionine.

suppressed *ACSL4* expression (Fig. 5C) and impaired HT1080 cell proliferation (Fig. 5D), while not inducing ferroptosis (Fig. 5E and F); however, it has a certain inducing effect on apoptosis (Fig. 5G). Taken together, these results establish methionine as an essential metabolic requirement for tumor cell proliferation, operating through ACSL4-mediated lipid metabolic pathways.

Discussion

Amino acid metabolism serves as a critical metabolic hub supporting the biosynthetic and energetic demands of rapidly proliferating tumor cells. Among the essential amino acids, methionine, a sulfur-containing metabolite with pleiotropic functions, has emerged as a promising therapeutic target in oncology (14,29). The present study identified a unique role for methionine in governing lipid homeostasis, demonstrating its superior capacity to modulate intracellular lipid accumulation and fatty acid uptake compared with other essential amino acids. Mechanistically, it was established that methionine exerts this control through SAM-dependent regulation of ACSL4, a master regulator of fatty acid metabolism (27). Downregulation of MAT2A, the rate-limiting enzyme in methionine-to-SAM conversion (24), phenocopied methionine deprivation by reducing lipid stores and impairing fatty acid internalization. Notably, these metabolic perturbations translated to significant anti-proliferative effects in tumor cells, highlighting the therapeutic potential of targeting methionine metabolism. Furthermore, methionine restriction has emerged as a promising therapeutic strategy in oncology, primarily through its depletion of SAM, the universal methyl donor critical for numerous cellular processes (30-32). The present study

extends this paradigm by revealing an additional mechanism whereby methionine restriction impairs tumor proliferation through ACSL4 downregulation-mediated inhibition of fatty acid uptake. The therapeutic potential of targeting methionine metabolism is further underscored by the frequent upregulation of MAT2A across diverse malignancies (33,34). In view of this, MAT2A has become an important target for cancer treatment, and inhibitors developed around it are constantly emerging (24,35,36). Notably, the MAT2A inhibitor, AG-270, has entered phase I clinical trials as a potential therapeutic agent for malignant tumors (24). Furthermore, ACSL4, a crucial enzyme in lipid metabolism regulation, has been demonstrated to facilitate metastatic extravasation in ovarian cancer through its enhancement of membrane fluidity and cellular invasiveness (37). Consequently, targeted disruption of the methionine-MAT2A-ACSL4 axis represents a potential therapeutic strategy to simultaneously suppress tumor proliferation and metastasis.

MAT2A is essential for maintaining intracellular SAM homeostasis. Emerging evidence indicates that the regulatory subunit, MAT2B, mediates SAM-dependent feedback inhibition of MAT2A activity (38-41). In addition, the present study extended these findings by demonstrating that: i) Methionine deprivation upregulates MAT2A expression; ii) SAM supplementation suppresses this induction; and iii) this regulatory mechanism operates independently of the methyltransferase activity of SAM. We hypothesize that mTORC1 may serve as a key mediator in SAM-dependent regulation of MAT2A expression. This speculation is supported by existing evidence demonstrating that mTORC1 can modulate MAT2A expression through its downstream effector, MYC (42). Furthermore, a study has suggested that SAM may exert feedback control on MAT2A through the SAM sensor, SAMTOR, which interfaces with both the mTORC1 and MYC signaling pathways (43). Therefore, the feedback regulation of MAT2A by SAM contributes to the steady-state of methionine-MAT2A-SAM.

ACSL4, a key regulator of lipid metabolism, catalyzes the ATP-dependent conversion of fatty acids to acyl-CoA esters. Extensive studies have established that ACSL4 governs cellular fatty acid uptake capacity by maintaining the intracellular acyl-CoA pool (44,45). The present study revealed that methionine deprivation decreased ACSL4 protein abundance, leading to impaired fatty acid internalization. In future research, the construction of isogenic ACSL4-knockout cell lines will be critical for characterizing ACSL4-dependent lipid metabolic pathways and for determining whether methionine restriction can further modulate intracellular lipid dynamics in ACSL4-deficient contexts. Notably, this lipid metabolic perturbation can be rescued by SAM supplementation, suggesting SAM-dependent regulation of ACSL4. However, the molecular mechanisms underlying SAM-mediated control of ACSL4 expression and activity require further investigation. Previous evidence provides important mechanistic insights into this regulatory process. A previous study demonstrated that SAM modulates mTORC1 activity through its sensor protein, SAMTOR (43). As a central nutrient-sensing hub, mTORC1 plays a pivotal role in coordinating cellular anabolism and metabolic reprogramming. Notably, mTORC1 has been shown to directly regulate ACSL4 expression (46). Based on these established relationships, we propose a model wherein SAM regulates ACSL4 levels through SAMTOR-mediated modulation of mTORC1 signaling activity.

As the primary product of the methionine-MAT2A-SAM metabolic axis, SAM serves as the universal methyl donor for diverse biological methylation reactions, including protein, DNA, RNA and small molecule modifications (47). Given this extensive substrate diversity, we hypothesize that the regulatory mechanisms by which the methionine-MAT2A-SAM axis influences ACSL4 and lipid metabolism remain incompletely characterized. Furthermore, the additional role of SAM as a precursor for polyamine biosynthesis (48) suggests potential cross-regulation between polyamine metabolism and ACSL4-mediated lipid pathways. Collectively, these observations highlight the multifaceted regulatory capacity of the methionine-MAT2A-SAM axis in cellular metabolism.

The present study has certain limitations. Notably, the BODIPY probe used in the present study functions as a broad-spectrum lipid stain, lacking molecular specificity. Consequently, while this method effectively detects overall lipid uptake, it does not discriminate between distinct lipid species. This represents a limitation of the current approach, as it precludes detailed characterization of the specific lipid subtypes involved in the observed processes.

In conclusion, the present study elucidated a novel regulatory mechanism by which methionine governs cellular lipid homeostasis through modulation of fatty acid uptake. These findings establish the methionine-MAT2A-SAM axis as a central metabolic regulator and reveal its therapeutic potential for targeted cancer interventions.

Acknowledgements

Not applicable.

Funding

The present study was supported by the Zhejiang Sci-Tech University Research Start-up Fund (grant no. 24042191-Y).

Availability of data and materials

The data generated in the present study may be requested from the corresponding author.

Authors' contributions

CX conceived the project, designed the research and led the entire experiment, from design to execution. JM assisted with the experiments. CX analyzed the data and wrote the manuscript. CX and JM confirm the authenticity of all the raw data. All authors have read and approved the final version of the manuscript.

Ethics approval and consent to participate

Not applicable.

Patient consent for publication

Not applicable.

Competing interests

The authors declare that they have no competing interests.

References

1. Cairns RA, Harris IS and Mak TW: Regulation of cancer cell metabolism. Nat Rev Cancer 11: 85-95, 2011.
2. Mossmann D, Park S and Hall MN: mTOR signalling and cellular metabolism are mutual determinants in cancer. Nat Rev Cancer 18: 744-757, 2018.
3. Wang W and Zou W: Amino acids and their transporters in T cell immunity and cancer therapy. Mol Cell 80: 384-395, 2020.
4. Yoneshiro T, Wang Q, Tajima K, Matsushita M, Maki H, Igarashi K, Dai Z, White PJ, McGarrah RW, Ilkayeva OR, *et al*: BCAA catabolism in brown fat controls energy homeostasis through SLC25A44. Nature 572: 614-619, 2019.
5. Gao X, Locasale JW and Reid MA: Serine and methionine metabolism: Vulnerabilities in lethal prostate cancer. Cancer Cell 35: 339-341, 2019.
6. Kelly B and Pearce EL: Amino assets: How amino acids support immunity. Cell Metab 32: 154-175, 202.
7. Labuschagne CF, van den Broek NJ, Mackay GM, Vousden KH and Maddocks OD: Serine, but not glycine, supports one-carbon metabolism and proliferation of cancer cells. Cell Rep 7: 1248-1258, 2014.
8. Longchamp A, Mirabella T, Arduini A, MacArthur MR, Das A, Treviño-Villarreal JH, Hine C, Ben-Sahra I, Knudsen NH, Brace LE, *et al*: Amino acid restriction triggers angiogenesis via GCN2/ATF4 regulation of VEGF and H(2)S production. Cell 173: 117-129.e14, 2018.
9. Knaus LS, Basilico B, Malzl D, Gerykova Bujalkova M, Smogavec M, Schwarz LA, Gorkiewicz S, Amberg N, Pauler FM, Knittl-Frank C, *et al*: Large neutral amino acid levels tune perinatal neuronal excitability and survival. Cell 186: 1950-1967.e25, 2023.
10. Handzlik MK, Gengatharan JM, Frizzi KE, McGregor GH, Martino C, Rahman G, Gonzalez A, Moreno AM, Green CR, Guernsey LS, *et al*: Insulin-regulated serine and lipid metabolism drive peripheral neuropathy. Nature 614: 118-124, 2023.
11. Zhang Y, Lin S, Peng J, Liang X, Yang Q, Bai X, Li Y, Li J, Dong W, Wang Y, *et al*: Amelioration of hepatic steatosis by dietary essential amino acid-induced ubiquitination. Mol Cell 82: 1528-1542.e10, 2022.
12. Schulte ML, Fu A, Zhao P, Li J, Geng L, Smith ST, Kondo J, Coffey RJ, Johnson MO, Rathmell JC, *et al*: Pharmacological blockade of ASCT2-dependent glutamine transport leads to antitumor efficacy in preclinical models. Nat Med 24: 194-202, 2018.
13. Muthusamy T, Cordes T, Handzlik MK, You L, Lim EW, Gengatharan J, Pinto AFM, Badur MG, Kolar MJ, Wallace M, *et al*: Serine restriction alters sphingolipid diversity to constrain tumour growth. Nature 586: 790-795, 2020.
14. Gao X, Sanderson SM, Dai Z, Reid MA, Cooper DE, Lu M, Richie JP Jr, Ciccarella A, Calcagnotto A, Mikhael PG, *et al*: Dietary methionine influences therapy in mouse cancer models and alters human metabolism. Nature 572: 397-401, 2019.
15. Mossmann D, Müller C, Park S, Ryback B, Colombi M, Ritter N, Weißenberger D, Dazert E, Coto-Llerena M, Nuciforo S, *et al*: Arginine reprograms metabolism in liver cancer via RBM39. Cell 186: 5068-5083.e23, 2023.
16. Krall AS, Mullen PJ, Surjono F, Momcilovic M, Schmid EW, Halbrook CJ, Thambundit A, Mittelman SD, Lyssiotis CA, Shackelford DB, *et al*: Asparagine couples mitochondrial respiration to ATF4 activity and tumor growth. Cell Metab 33: 1013-1026.e6, 2021.
17. Missiaen R, Anderson NM, Kim LC, Nance B, Burrows M, Skuli N, Carens M, Riscal R, Steensels A, Li F and Simon MC: GCN2 inhibition sensitizes arginine-deprived hepatocellular carcinoma cells to senolytic treatment. Cell Metab 34: 1151-1167.e7, 2022.
18. Badgley MA, Kremer DM, Maurer HC, DelGiorno KE, Lee HJ, Purohit V, Sagalovskiy IR, Ma A, Kapilian J, Firl CEM, *et al*: Cysteine depletion induces pancreatic tumor ferroptosis in mice. Science 368: 85-89, 2020.
19. Xue Y, Lu F, Chang Z, Li J, Gao Y, Zhou J, Luo Y, Lai Y, Cao S, Li X, *et al*: Intermittent dietary methionine deprivation facilitates tumoral ferroptosis and synergizes with checkpoint blockade. Nat Commun 14: 4758, 2023.
20. Zheng J and Conrad M: The metabolic underpinnings of ferroptosis. Cell Metab 32: 920-937, 2020.
21. Zhang W, Li Q, Zhang Y, Wang Z, Yuan S, Zhang X, Zhao M, Zhuang W and Li B: Multiple myeloma with high expression of SLC7A11 is sensitive to erastin-induced ferroptosis. Apoptosis 29: 412-423, 2024.
22. Koppula P, Zhuang L and Gan B: Cystine transporter SLC7A11/xCT in cancer: Ferroptosis, nutrient dependency, and cancer therapy. Protein Cell 12: 599-620, 2021.
23. Dixon SJ, Patel DN, Welsch M, Skouta R, Lee ED, Hayano M, Thomas AG, Gleason CE, Tatonetti NP, Slusher BS and Stockwell BR: Pharmacological inhibition of cystine-glutamate exchange induces endoplasmic reticulum stress and ferroptosis. Elife 3: e02523, 2014.
24. Gounder M, Johnson M, Heist RS, Shapiro GI, Postel-Vinay S, Wilson FH, Garralda E, Wulf G, Almon C, Nabhan S, *et al*: MAT2A inhibitor AG-270/S095033 in patients with advanced malignancies: A phase I trial. Nat Commun 16: 423, 2025.
25. Cacciatore A, Shinde D, Musumeci C, Sandrini G, Guarrera L, Albino D, Civenni G, Storelli E, Mosole S, Federici E, *et al*: Epigenome-wide impact of MAT2A sustains the androgen-indifferent state and confers synthetic vulnerability in ERG fusion-positive prostate cancer. Nat Commun 15: 6672, 2024.
26. Hou PP, Zheng CM, Wu SH, Liu XX, Xiang GX, Cai WY, Chen G and Lou YL: Extracellular vesicle-packaged ACSL4 induces hepatocyte senescence to promote hepatocellular carcinoma progression. Cancer Res 84: 3953-3966, 2024.
27. Doll S, Proneth B, Tyurina YY, Panzilius E, Kobayashi S, Ingold I, Irmler M, Beckers J, Aichler M, Walch A, *et al*: ACSL4 dictates ferroptosis sensitivity by shaping cellular lipid composition. Nat Chem Biol 13: 91-98, 2017.
28. Chaneton B, Hillmann P, Zheng L, Martin ACL, Maddocks ODK, Chokkathukalam A, Coyle JE, Jankevics A, Holding FP, Vousden KH, *et al*: Serine is a natural ligand and allosteric activator of pyruvate kinase M2. Nature 491: 458-462, 2012.
29. Cunningham A, Erdem A, Alshamleh I, Geugien M, Pruis M, Pereira-Martins DA, van den Heuvel FAJ, Wierenga ATJ, Ten Berge H, Dennebos R, *et al*: Dietary methionine starvation impairs acute myeloid leukemia progression. Blood 140: 2037-2052, 2022.
30. Wang QL, Chen Z, Lu X, Lin H, Feng H, Weng N, Chen L, Liu M, Long L, Huang L, *et al*: Methionine metabolism dictates PCSK9 expression and antitumor potency of PD-1 blockade in MSS colorectal cancer. Adv Sci (Weinh) 12: e2501623, 2025.
31. Hong XL, Huang CK, Qian H, Ding CH, Liu F, Hong HY, Liu SQ, Wu SH, Zhang X and Xie WF: Positive feedback between arginine methylation of YAP and methionine transporter SLC43A2 drives anticancer drug resistance. Nat Commun 16: 87, 2025.
32. Zhang X, Zhao Z, Wang X, Zhang S, Zhao Z, Feng W, Xu L, Nie J, Li H, Liu J, *et al*: Deprivation of methionine inhibits osteosarcoma growth and metastasis via C1orf112-mediated regulation of mitochondrial functions. Cell Death Dis 15: 349, 2024.
33. Huang Z, Chen P and Liu Y: RBM15-mediated the m6A modification of MAT2A promotes osteosarcoma cell proliferation, metastasis and suppresses ferroptosis. Mol Cell Biochem 480: 2923-2933, 2025.
34. Xia S, Liang Y, Shen Y, Zhong W and Ma Y: MAT2A inhibits the ferroptosis in osteosarcoma progression regulated by miR-26b-5p. J Bone Oncol 41: 100490, 2023.
35. Yang S, Gu X, Chen L and Zhu W: Discovery of novel spirocyclic MAT2A inhibitors demonstrating high in vivo efficacy in MTAP-Null xenograft models. J Med Chem 68: 3480-3494, 2025.
36. Zhou Y, Wang L, Ren R, Zhang J, Huan X, Yang P, Miao ZH, Xiong B, Wang Y and Liu T: Structure-based discovery of a series of novel MAT2a inhibitors. ACS Med Chem Lett 16: 646-650, 2025.
37. Wang Y, Hu M, Cao J, Wang F, Han JR, Wu TW, Li L, Yu J, Fan Y, Xie G, *et al*: ACSL4 and polyunsaturated lipids support metastatic extravasation and colonization. Cell 188: 412-429.e27, 2025.
38. Shafqat N, Muniz JR, Pilka ES, Papagrigoriou E, von Delft F, Oppermann U and Yue WW: Insight into S-adenosylmethionine biosynthesis from the crystal structures of the human methionine adenosyltransferase catalytic and regulatory subunits. Biochem J 452: 27-36, 2013.
39. LeGros HL Jr, Halim AB, Geller AM and Kotb M: Cloning, expression, and functional characterization of the beta regulatory subunit of human methionine adenosyltransferase (MAT II). J Biol Chem 275: 2359-2366, 2000.

40. LeGros L, Halim AB, Chamberlin ME, Geller A and Kotb M: Regulation of the human MAT2B gene encoding the regulatory beta subunit of methionine adenosyltransferase, MAT II. J Biol Chem 276: 24918-24924, 2001.
41. Li Z, Wang F, Liang B, Su Y, Sun S, Xia S, Shao J, Zhang Z, Hong M, Zhang F and Zheng S: Methionine metabolism in chronic liver diseases: An update on molecular mechanism and therapeutic implication. Signal Transduct Target Ther 5: 280, 2020.
42. Villa E, Sahu U, O'Hara BP, Ali ES, Helmin KA, Asara JM, Gao P, Singer BD and Ben-Sahra I: mTORC1 stimulates cell growth through SAM synthesis and m^6A mRNA-dependent control of protein synthesis. Mol Cell 81: 2076-2093.e9, 2021.
43. Gu X, Orozco JM, Saxton RA, Condon KJ, Liu GY, Krawczyk PA, Scaria SM, Harper JW, Gygi SP and Sabatini DM: SAMTOR is an S-adenosylmethionine sensor for the mTORC1 pathway. Science 358: 813-818, 2017.
44. Ibrahim A, Yucel N, Kim B and Arany Z: Local mitochondrial ATP production regulates endothelial fatty acid uptake and transport. Cell Metab 32: 309-319.e7, 2020.
45. Milger K, Herrmann T, Becker C, Gotthardt D, Zickwolf J, Ehehalt R, Watkins PA, Stremmel W and Füllekrug J: Cellular uptake of fatty acids driven by the ER-localized acyl-CoA synthetase FATP4. J Cell Sci 119: 4678-4688, 2006.
46. Huang B, Nie G, Dai X, Cui T, Pu W and Zhang C: Environmentally relevant levels of Cd and Mo coexposure induces ferroptosis and excess ferritinophagy through AMPK/mTOR axis in duck myocardium. Environ Toxicol 39: 4196-4206, 2024.
47. Ouyang Y, Wu Q, Li J, Sun S and Sun S: S-adenosylmethionine: A metabolite critical to the regulation of autophagy. Cell Prolif 53: e12891, 2020.
48. Fernández-Ramos D, Lopitz-Otsoa F, Lu SC and Mato JM: S-adenosylmethionine: A multifaceted regulator in cancer pathogenesis and therapy. Cancers (Basel) 17: 535, 2025.